

The binding energy parameter for common envelope evolution

Chen Wang, Kun Jia and Xiang-Dong Li

Department of Astronomy, Nanjing University, Nanjing 210046, China; lixd@nju.edu.cn
 Key Laboratory of Modern Astronomy and Astrophysics (Nanjing University), Ministry of Education, Nanjing 210046, China

Received 2016 March 28; accepted 2016 April 20

Abstract The binding energy parameter λ plays a vital role in common envelope evolution. Though it is well known that λ takes different values for stars with different masses and varies during stellar evolution, it has been erroneously adopted as a constant in most population synthesis calculations. We have systematically calculated the values of λ for stars of masses $1 - 60 M_{\odot}$ by use of an updated stellar evolution code, taking into account the contribution from both gravitational energy and internal energy to the binding energy of the envelope. We adopt the criterion for the core-envelope boundary advocated by Ivanova. A new kind of λ with an enthalpy prescription is also investigated. We present fitting formulae for the calculated values of various kinds of λ , which can be used in future population synthesis studies.

Key words: binaries: general — stars: evolution — stars: mass-loss

1 INTRODUCTION

Common envelope (CE) evolution is one of the most important and yet unresolved stages in the formation of various types of binary systems including low-mass X-ray binaries and cataclysmic variables. For semi-detached binaries, mass transfer can be dynamically unstable if the mass ratio is larger than a critical value or the envelope of the donor star is in convective equilibrium. In this case, the accreting star, usually the less massive star, cannot maintain thermal equilibrium, and the transferred material accumulates on its surface. As a result, both components are expected to overflow their respective Roche lobes (RLs), forming an envelope enshrouding both stars. The accreting star then spirals into the donor's envelope, using its orbital energy to expel the envelope. This is the so-called CE evolution (see Iben & Livio 1993; Taam & Sandquist 2000; Ivanova et al. 2013 for reviews). The outcome of CE evolution is either a compact binary consisting of the donor's core and the companion star, or a single object due to merger of the two stars, depending on whether the available orbital energy is large enough to eject the donor's envelope. This process can be described by the following equation (Webbink 1984),

$$E_{\text{bind}} = \alpha_{\text{CE}} \left(\frac{GM_{\text{core}}M_2}{2a_f} - \frac{GM_1M_2}{2a_i} \right), \quad (1)$$

where

$$E_{\text{bind}} = - \int_{M_{\text{core}}}^{M_1} \frac{GM(r)}{r} dm \quad (2)$$

is the binding energy of the envelope, α_{CE} the efficiency parameter that denotes the fraction of the orbital energy used to eject the CE, G the gravitational constant, M_1 and M_{core} the masses of the donor and its core respectively, M_2 the mass of the companion star, and a_i and a_f the pre- and post-CE orbital separations respectively.

It has been suggested that the internal energy (including both thermal and recombination energies) in the envelope may also contribute to the binding energy, so a more general form for E_{bind} can be written as

$$E_{\text{bind}} = \int_{M_{\text{core}}}^{M_1} \left[-\frac{GM(r)}{r} + U \right] dm, \quad (3)$$

where U is the internal energy (Han et al. 1994; Dewi & Tauris 2000). More recently, Ivanova & Chaichenets (2011) proposed that this canonical energy formalism should be modified with an additional P/ρ term (where P is the pressure and ρ is the density of gas) by taking into account the mass outflows during the spiral-in stage. These authors argue that the standard form (1) or (2) is based on the consideration that the envelope of a giant star is dispersed or unstable once its total energy $W_{\text{env}} > 0$, but neither of the two considerations has to occur when the envelope has quasi-steady outflows. For such envelopes, the material obeys the first law of thermodynamics, and the criterion for a mass shell to reach the point of no return in its expansion turns out to be that the sum of its kinetic energy, potential energy and enthalpy, rather than the total energy, becomes positive. This is the so-called enthalpy model (see Ivanova et al. 2013 for a detailed discussion). Assuming that the velocity of gas at infinity is zero, the

binding energy is expressed as

$$E_{\text{bind}} = \int_{M_{\text{core}}}^{M_1} \left[-\frac{GM(r)}{r} + U + \frac{P}{\rho} \right] dm. \quad (4)$$

Since the P/ρ term is always non-negative and orders of magnitude larger than U , the absolute value of E_{bind} decreases substantially in this case. One should be cautious that quasi-stationary mass outflow only develops when the envelope experiences a slow self-regulated phase during the spiral-in stage, that is, the spiral-in phase proceeds on a thermal timescale (Ivanova et al. 2013).

de Kool (1990) proposed a convenient way to evaluate the binding energy by introducing a parameter λ for characterizing the central concentration of the donor's envelope,

$$E_{\text{bind}} = -\frac{GM_1 M_{\text{env}}}{\lambda a_i r_L}, \quad (5)$$

where $M_{\text{env}} = M_1 - M_{\text{core}}$ is the mass of the envelope, and $r_L = R_L/a_i$ is the ratio of the donor's RL radius to the orbital separation at the onset of CE evolution. Typically, $a_i r_L$ is taken to be the stellar radius once a star fills its RL. Thus the post-CE separation can be determined by inserting Equation (5) into Equation (1),

$$\frac{a_f}{a_i} = \frac{M_{\text{core}} M_2}{M_1} \frac{1}{M_2 + 2M_{\text{env}}/\alpha_{\text{CE}} \lambda r_L}. \quad (6)$$

It should be emphasized that both α_{CE} and λ are variables depending on stellar and binary parameters, although they have been treated as constant (< 1) in most of the population synthesis calculations, due to both poor understanding of them and convenience for calculation. However, many studies (e.g. Dewi & Tauris 2000; Podsiadlowski et al. 2003; Webbink 2008; Xu & Li 2010a,b; Wong et al. 2014) have shown that λ varies as the star evolves and can deviate far from a constant value (say 0.5). Some investigations also suggested that α_{CE} may depend on the binary parameters such as the component mass and the orbital period (e.g., Taam & Sandquist 2000; Podsiadlowski et al. 2003; De Marco et al. 2011; Davis et al. 2012).

Systematic calculations of the values of λ have been performed by Dewi & Tauris (2000), Podsiadlowski et al. (2003) and Xu & Li (2010a,b). In the latter, fitting formulae for λ have also been provided so they can be incorporated into population synthesis investigations. In this work we re-visit this problem and provide more reliable λ values by taking into account the following factors.

First, we adopt the Modules for Experiments in Stellar Astrophysics (MESA) code (Paxton et al. 2011, 2013, 2015) to calculate stellar evolution, which is more powerful in probing the stellar structure than Eggleton (1971)'s evolution code EV previously adopted by Xu & Li (2010a,b). Employing modern software engineering tools and techniques allows MESA to consistently evolve stellar models through challenging phases for stellar evolution codes in the past, for example, the He core flash in low-mass stars and advanced nuclear burning in massive stars

(Paxton et al. 2011). It also adopts denser grids for stellar structure than the EV code. We find that stars appear to be generally less compact after evolving off the main sequence when modeled with MESA compared with the EV code. The structure of the hydrogen-burning shell, which is near the defined core-envelope boundary, plays a vital role in determining the value of λ .

Second, besides the traditional λ related to gravitational energy and internal energy, we also calculate the values of λ in the enthalpy prescription.

Third, it is well known that the λ -value is sensitive to the definition of the core-envelope boundary (see Ivanova et al. 2013 for a detailed discussion). It was arbitrarily assumed to be the (10% – 15%) hydrogen layer in Dewi & Tauris (2000) and Xu & Li (2010a). Ivanova (2011) proposed that this boundary should be defined in the hydrogen shell which has the maximum local sonic velocity (i.e., the maximal compression) prior to CE evolution. This criterion comes from the study of the outcome of the CE event and the fact that a helium core would experience a post-CE thermal readjustment phase, and presents a more self-consistent definition of the core-envelope boundary.

This paper is organized as follows. In Section 2, we briefly describe the stellar models and assumptions adopted. We present the calculated results and fitting formulae for λ in Section 3. Our conclusions are in Section 4.

2 MODEL DESCRIPTION

We adopted an updated version (7624) of the MESA code to calculate the binding energy parameter λ for stars with initial masses in the range of $1 - 60 M_{\odot}$. We consider Pop. I stars with the chemical compositions of $X = 0.7$ and $Z = 0.02$. Our previous study has shown that there is not a significant change in the values of λ for Pop. I and II stars (Xu & Li 2010a,b).

It has been recognized that stellar winds play an important role in determining the λ parameter, especially for massive stars (Podsiadlowski et al. 2003). Here, we adopt two prescriptions for the wind mass loss rates. The first one, denoted as Wind1, is the same as in Hurley et al. (2000) and Vink et al. (2001) (for O and B stars), and the second, denoted as Wind2, takes the maximum value of the above loss rates in all the evolutionary stages, to be consistent with Xu & Li (2010a,b).

The Wind1 prescription is described as follows:

- (1) Stellar wind mass loss described by Nieuwenhuijzen & de Jager (1990):

$$\dot{M}_{\text{NJ}}(M_{\odot} \text{ yr}^{-1}) = 9.6 \times 10^{-15} R^{0.81} L^{1.24} M^{0.16}, \quad (7)$$

where M , R and L are the stellar mass, radius and luminosity in solar units, respectively.

- (2) Wind loss from giant branch stars by Kudritzki & Reimers (1978):

$$\dot{M}_{\text{R}}(M_{\odot} \text{ yr}^{-1}) = 2 \times 10^{-13} \frac{LR}{M}. \quad (8)$$

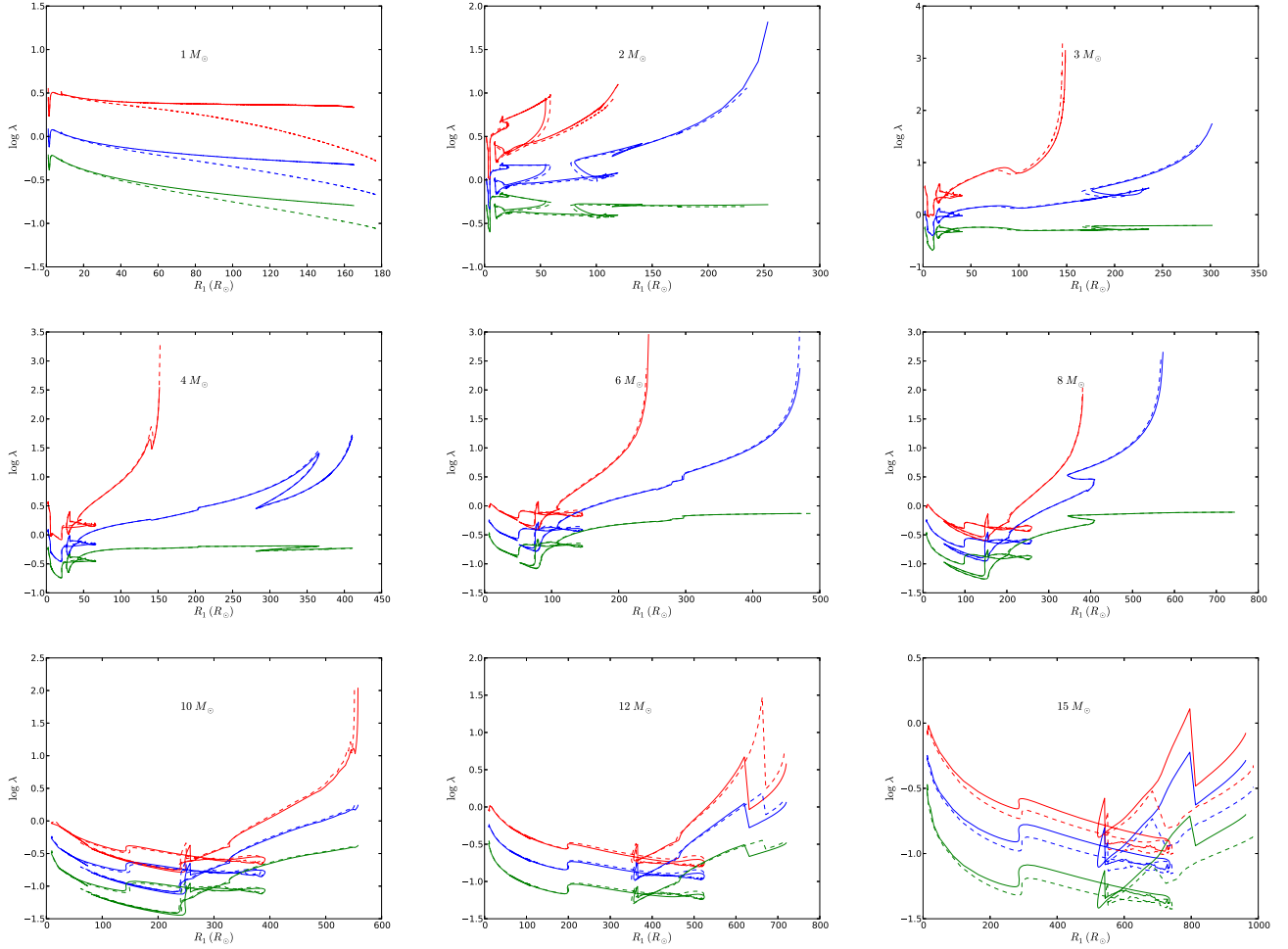


Fig. 1 Evolution of the binding energy parameters λ with the stellar radius R for $1 - 15 M_{\odot}$ stars. The red, blue and green lines represent λ_h , λ_b and λ_g respectively, and the solid and dashed lines represent the results with the Wind1 and Wind2 prescriptions respectively.

- (3) Wind loss from asymptotic giant branch (AGB) stars by Vassiliadis & Wood (1993):

$$\log \dot{M}_{\text{VW}} (M_{\odot} \text{ yr}^{-1}) = -11.4 + 0.0125 \times [P_0 - 100 \max(M - 2.5, 0.0)], \quad (9)$$

where

$$\log P_0 = \min(3.3, -2.07 - 0.9 \log M + 1.94 \log R). \quad (10)$$

The maximum wind loss rate in this prescription is limited to

$$\dot{M}_{\text{VW,max}} = 1.36 \times 10^{-9} L M_{\odot} \text{ yr}^{-1}. \quad (11)$$

- (4) Wolf-Rayet-like mass loss by Hamann et al. (1995) and Hamann & Koesterke (1998):

$$\dot{M}_{\text{WR}} (M_{\odot} \text{ yr}^{-1}) = 10^{-13} L^{1.5} (1.0 - \mu) M_{\odot} \text{ yr}^{-1}, \quad (12)$$

with

$$\mu = \left(\frac{M - M_{\text{core}}}{M} \right) \min \times \left\{ 5.0, \max \left[1.2, \left(\frac{L}{L_0} \right)^{\kappa} \right] \right\}, \quad (13)$$

where $L_0 = 7.0 \times 10^4$ and $\kappa = -0.5$.

- (5) The wind loss of O and B type stars according to Vink et al. (2001):

$$\begin{aligned} \log \dot{M}_{\text{OB}} (M_{\odot} \text{ yr}^{-1}) = & -6.697 (\pm 0.061) + 2.194 (\pm 0.021) \log(L/10^5) \\ & -1.313 (\pm 0.046) \log(M/30) \\ & -1.226 (\pm 0.037) \log\left(\frac{v_{\infty}/v_{\text{esc}}}{2.0}\right) \\ & +0.933 (\pm 0.064) \log(T_{\text{eff}}/40000) \\ & -10.92 (\pm 0.90) \log(T_{\text{eff}}/40000)^2, \end{aligned}$$

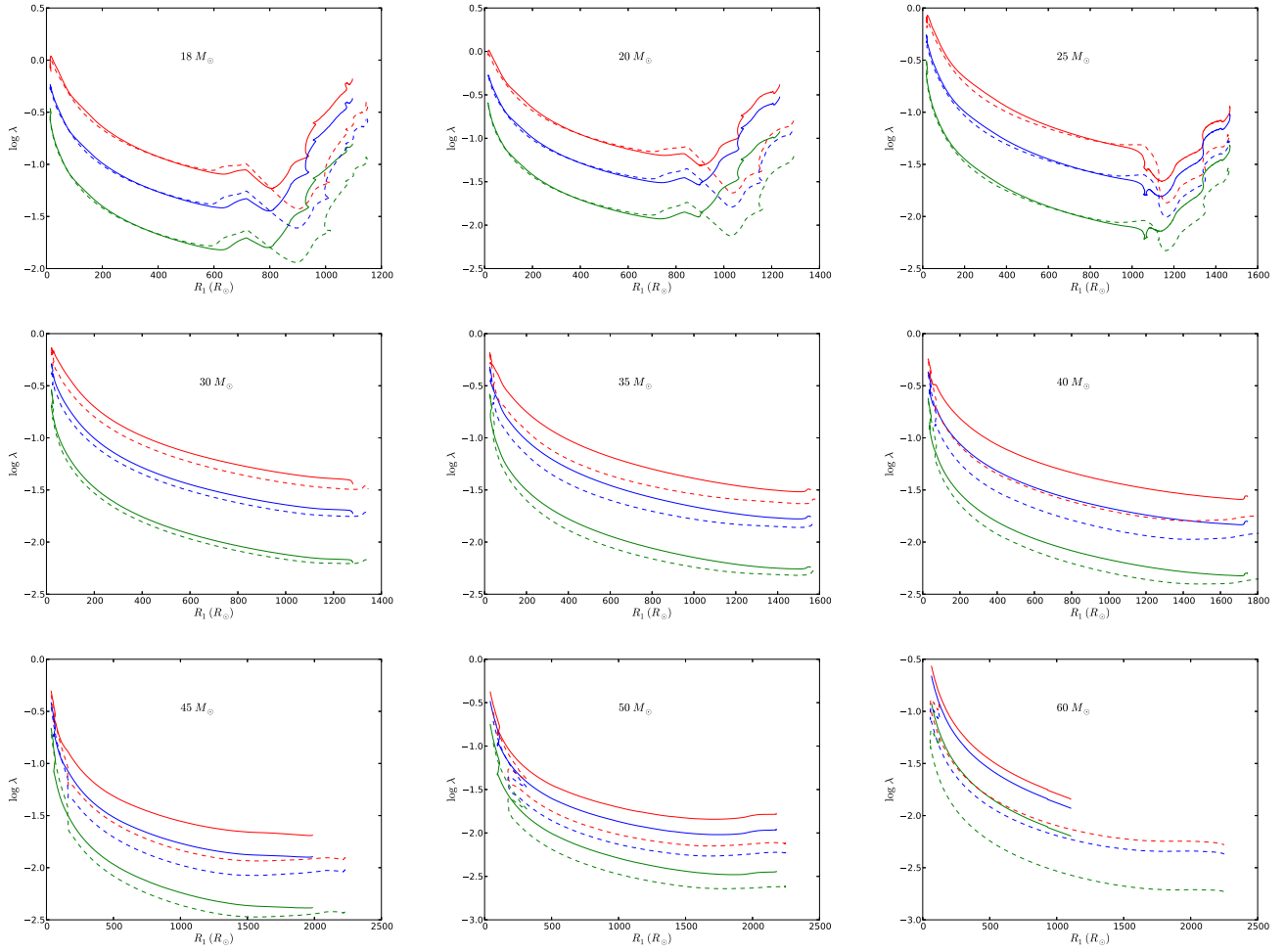


Fig. 2 Same as Fig. 1 but for 18 – 60 M_{\odot} stars.

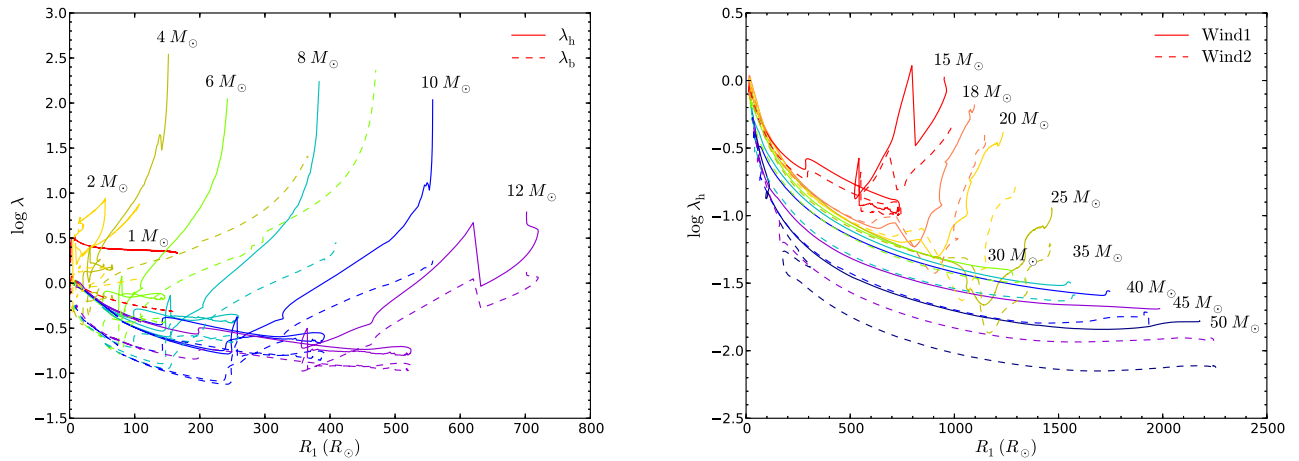


Fig. 3 Comparison of the values of λ for different stars. In the left panel, the solid and dashed lines represent λ_h and λ_b for stars less massive than $15 M_{\odot}$ with the Wind1 prescription, respectively. The right panel shows λ_h as a function of the stellar radius for stars more massive than $15 M_{\odot}$. The solid and dashed lines represent the results with the Wind1 and Wind2 prescriptions, respectively.

with $v_\infty/v_{\text{esc}} = 2.6$ for $27\,500\text{ K} < T_{\text{eff}} \leq 50\,000\text{ K}$ (where T_{eff} is the effective temperature).

$$\begin{aligned} \log \dot{M}_{\text{OB}}(M_\odot \text{ yr}^{-1}) = & \\ & -6.688(\pm 0.080) + 2.210(\pm 0.031) \log(L/10^5) \\ & -1.339(\pm 0.068) \log(M/30) \\ & -1.601(\pm 0.055) \log\left(\frac{v_\infty/v_{\text{esc}}}{2.0}\right) \\ & +1.07(\pm 0.10) \log(T_{\text{eff}}/20\,000), \end{aligned}$$

with $v_\infty/v_{\text{esc}} = 1.3$ for $12\,500\text{ K} \leq T_{\text{eff}} \leq 22\,500\text{ K}$.

The mass loss in the Wind2 prescription is taken to be

$$\dot{M} = \max(\dot{M}_{\text{NJ}}, \dot{M}_{\text{R}}, \dot{M}_{\text{VW}}, \dot{M}_{\text{WR}}, \dot{M}_{\text{OB}}). \quad (14)$$

We ignore the effect of stellar rotation in the calculation, because CE evolution usually occurs when the donor star has already entered the giant phase with slow rotation.

3 RESULTS AND DISCUSSION

We have calculated the values of different λ s for $1\text{--}60 M_\odot$ stars by combining Equations (2)–(5), considering gravitational binding energy alone, total energy, and total energy plus enthalpy in the stellar envelope separately. We denote them as λ_g , λ_b and λ_h , respectively, that is,

$$\begin{aligned} -\frac{GM_1 M_{\text{env}}}{\lambda_g a_i r_L} &= -\int_{M_{\text{core}}}^{M_1} \frac{GM(r)}{r} dm, \\ -\frac{GM_1 M_{\text{env}}}{\lambda_b a_i r_L} &= \int_{M_{\text{core}}}^{M_1} \left[-\frac{GM(r)}{r} + U \right] dm, \end{aligned}$$

and

$$-\frac{GM_1 M_{\text{env}}}{\lambda_h a_i r_L} = \int_{M_{\text{core}}}^{M_1} \left[-\frac{GM(r)}{r} + U + \frac{P}{\rho} \right] dm.$$

More massive stars may lose most of their envelope through strong winds so CE evolution is not likely to occur. For each star, we follow its evolution until it ascends the thermally pulsating AGB where the star initiates repeated expansions and contractions (for stars $> 4 M_\odot$), or the code discontinues execution automatically. The binding energy between the envelope and the maximum compression point in the hydrogen burning shell is calculated once a star evolves to produce such a shell. Here, the maximum compression point is the place with the highest local sonic velocity (i.e., the largest value for P/ρ in the shell).

Figures 1 and 2 show the evolution of λ s with respect to the stellar radius R for stars with different masses. The solid and dashed lines represent the results under the Wind1 and Wind2 prescriptions, respectively. The green, blue and red lines correspond to λ_g , λ_b and λ_h respectively in each case. In general they demonstrate a similar evolutionary trend, with λ_b being roughly twice as large as λ_g , which is a natural consequence of the Virial theorem, and λ_h being several times larger than λ_b . For stars with mass $\sim 1 M_\odot$ or $> 30 M_\odot$, λ s constantly decrease along the

evolutionary tracks, while for stars with mass in between, λ s decrease with increasing R at first and then increase when they have ascended the AGB and developed a deep convective envelope (see also Podsiadlowski et al. 2003). Most interestingly, for $\sim 3\text{--}10 M_\odot$ stars, λ_h (and λ_b in some cases) drastically increases in the supergiant phase, and can reach a “boiling pot” zone (see Han et al. 1994; Ivanova 2011), where the binding energy becomes positive before it expands to reach the maximum radius.

The differences between the solid and dashed lines demonstrate the influence of wind loss on the mass and the compactness of the envelope, especially near the core-envelope boundary. We can see that for stars of mass $\lesssim 15 M_\odot$ (except $1 M_\odot$), or stars of mass $\sim 15\text{--}30 M_\odot$ but with radius $\lesssim 500\text{--}1000 R_\odot$, the λ -values in the Wind1 case roughly coincide with those in the Wind2 case, reflecting that the two prescriptions are almost the same in such situations. In other cases, the λ -values in the Wind2 case are usually smaller than in the Wind1 case because of the steeper density profile in the envelope (see also Podsiadlowski et al. 2003).

To see how the binding energy changes with stellar mass, we compare λ_h and λ_b as a function of R for stars with different masses in Figure 3. Generally more massive stars have smaller λ , implying that ejection of the envelope is more difficult. This feature is particularly important for the formation of black hole low-mass X-ray binaries (Justham et al. 2006; Wang et al. 2016, and references there in).

In general, our calculated binding energy parameters λ_g and λ_b evolve in a way that agrees with previous studies. However, there are some remarkable differences in specific circumstances.

- (1) Compared with Xu & Li (2010a,b), we find that for $2\text{--}8 M_\odot$ stars the values of λ_g and λ_b increase more rapidly with radius during the AGB stage. For example, for a $3 M_\odot$ star, $\lambda_b \simeq 10$ at $300 R_\odot$ in Xu & Li (2010a,b), but $\simeq 100$ in our case.
- (2) Our calculations show that the λ -values increase with radius at the very end of the evolutionary stages for stars less massive than $\sim 30 M_\odot$ (except for a $1 M_\odot$ star), but this upper mass limit becomes lower, i.e., $\sim 20 M_\odot$ in Xu & Li (2010a,b) and Podsiadlowski et al. (2003).
- (3) The λ -values do not show a significant decline at the very end of the evolution for stars more massive than $\sim 30 M_\odot$ as observed by Podsiadlowski et al. (2003).

Finally, similar to Xu & Li (2010a,b) we perform polynomial fitting for the calculated λ -values,

$$\begin{aligned} \log \lambda = & a_0 + a_1 x + a_2 x^2 + a_3 x^3 + a_4 x^4 \\ & + a_5 x^5 + a_6 x^6, \end{aligned} \quad (15)$$

where $x = R/R_\odot$. For $2\text{--}15 M_\odot$ stars that have “hook”-like features in λ , we divide their post main sequence evolution into three stages, and fit the λ -values separately.

Table 1 Fitting Parameters for λ

Mass (M_{\odot})	Wind loss	Stage	λ	a_0	a_1	a_2	a_3	a_4	a_5	a_6	
1	Wind1		λ_h	0.439377368	0.006334748	-4.60E-04	1.05E-05	-1.11E-07	5.51E-10	-1.05E-12	
			λ_b	0.047486107	-0.001813814	-0.000202148	5.51E-06	-6.12E-08	3.13E-10	-6.06E-13	
			λ_g	-0.229504942	-0.006642966	-7.90E-05	3.36E-06	-4.09E-08	2.18E-10	-4.30E-13	
	Wind2		λ_h	0.446551051	0.004283965	-0.000362559	7.71E-06	-7.78E-08	3.68E-10	-6.63E-13	
			λ_b	0.051723323	-0.003092511	-0.000145916	3.91E-06	-4.21E-08	2.05E-10	-3.78E-13	
			λ_g	-0.226240947	-0.007668935	-3.70E-05	2.17E-06	-2.67E-08	1.37E-10	-2.60E-13	
2	Wind1	1	λ_h	0.458299689	-0.066491722	0.012809574	-0.00079697	2.35E-05	-3.33E-07	1.83E-09	
			λ_b	-0.055628327	-0.020278881	0.006650167	-0.000473348	1.49E-05	-2.18E-07	1.23E-09	
			λ_g	-0.365205393	-0.008048466	0.004718683	-0.000366995	1.19E-05	-1.79E-07	1.02E-09	
		2	λ_h	1.503848844	-0.307827791	0.033926633	-0.001915136	5.72E-05	-8.51E-07	4.97E-09	
			λ_b	0.078894909	-0.017355261	0.001880501	-0.000145636	5.81E-06	-1.06E-07	7.16E-10	
			λ_g	-0.318594414	0.01353053	-0.001715174	6.52E-05	-7.02E-07	-6.60E-09	1.24E-10	
		3	λ_h	0.80094725	-0.088162823	0.005190546	-0.000134579	1.77E-06	-1.14E-08	2.90E-11	
			λ_b	0.042516824	-0.017189807	0.000736229	-1.26E-05	1.02E-07	-3.85E-10	5.44E-13	
			λ_g	-0.278858406	-0.011175318	0.000408553	-6.72E-06	5.31E-08	-1.95E-10	2.66E-13	
	3	Wind1	1	λ_h	1.32158616	-0.511107713	0.069798235	-0.004234453	0.000129527	-1.96E-06	1.16E-08
				λ_b	0.553601499	-0.322402445	0.041379969	-0.002281134	6.15E-05	-7.87E-07	3.71E-09
				λ_g	0.147496542	-0.255352018	0.031009238	-0.001567046	3.67E-05	-3.63E-07	8.52E-10
		2	λ_h	-34.47232944	8.284562942	-0.792027265	0.039213067	-0.001063886	1.50E-05	-8.66E-08	
			λ_b	-21.26420026	4.998641287	-0.47435718	0.023385099	-0.000633095	8.94E-06	-5.15E-08	
			λ_g	-17.03794141	3.912297317	-0.369651011	0.018176049	-0.000491475	6.94E-06	-4.00E-08	
		3	λ_h	1.761358786	-0.210912284	0.010365416	-0.000222355	2.40E-06	-1.29E-08	2.73E-11	
			λ_b	-0.304912365	0.016425641	-0.000214159	9.87E-07	1.30E-09	-2.05E-11	3.98E-14	
			λ_g	-0.556787574	0.013693598	-0.000219799	1.53E-06	-4.85E-09	5.74E-12	5.16E-17	
4		Wind1	1	λ_h	1.060028729	-0.259126108	0.021464041	-0.000824166	1.64E-05	-1.63E-07	6.48E-10
				λ_b	0.396069457	-0.160359901	0.010528477	-0.000277383	2.93E-06	-4.06E-09	-7.92E-11
				λ_g	0.030959831	-0.128292612	0.006840813	-9.09E-05	-1.69E-06	5.09E-08	-3.31E-10
		2	λ_h	-158.2144537	21.3665151	-1.175629306	0.033828851	-0.000537603	4.48E-06	-1.53E-08	
			λ_b	-113.5126224	15.15018357	-0.827530643	0.023676471	-0.000374536	3.11E-06	-1.06E-08	
			λ_g	-95.30490909	12.61279533	-0.686025008	0.019562306	-0.000308629	2.56E-06	-8.69E-09	
		3	λ_h	6.21658444	-0.610564473	0.022771632	-0.000409896	3.88E-06	-1.86E-08	3.55E-11	
			λ_b	-0.865298169	0.023395321	-0.000167028	2.40E-07	2.51E-09	-1.07E-11	1.22E-14	
			λ_g	-1.318602631	0.035303846	-0.000452023	2.89E-06	-9.71E-09	1.63E-11	-1.08E-14	
	6	Wind1	1	λ_h	-0.080220619	0.018717693	-0.001599316	4.43E-05	-5.53E-07	3.21E-09	-7.08E-12
				λ_b	-0.181116753	-0.007930443	-0.000669357	2.93E-05	-4.24E-07	2.63E-09	-6.00E-12
				λ_g	-0.333386602	-0.022017403	-0.00015568	2.03E-05	-3.38E-07	2.21E-09	-5.17E-12
		2	λ_h	73.5586189	-4.777609245	0.124527396	-0.001679558	1.24E-05	-4.79E-08	7.56E-11	
			λ_b	77.90321325	-4.981465802	0.126967686	-0.001673014	1.21E-05	-4.56E-08	7.05E-11	
			λ_g	77.71103944	-4.947175949	0.124917607	-0.001629579	1.17E-05	-4.36E-08	6.66E-11	
		3	λ_h	6.445886556	-0.314136789	0.005644353	-5.18E-05	2.67E-07	-7.40E-10	8.60E-13	
			λ_b	1.958799141	-0.11166705	0.001646683	-1.08E-05	3.63E-08	-6.01E-11	3.92E-14	
			λ_g	0.571516609	-0.06864172	0.001021307	-6.51E-06	2.08E-08	-3.27E-11	2.02E-14	
8		Wind1	1	λ_h	-0.035692021	0.005572222	-0.000485211	8.19E-06	-5.94E-08	1.97E-10	-2.46E-13
				λ_b	-0.167246715	-0.00963629	-0.000147715	4.83E-06	-4.17E-08	1.50E-10	-1.95E-13
				λ_g	-0.332644809	-0.019069101	6.84E-05	2.52E-06	-2.87E-08	1.12E-10	-1.52E-13
		2	λ_h	-2.365068424	0.124227402	-0.002735286	2.83E-05	-1.50E-07	3.93E-10	-4.04E-13	
			λ_b	-4.533738779	0.212107478	-0.004366164	4.29E-05	-2.17E-07	5.44E-10	-5.37E-13	
			λ_g	-5.641282203	0.250488572	-0.005065902	4.90E-05	-2.44E-07	6.02E-10	-5.86E-13	
		3	λ_h	0.414442304	-0.025433442	0.000380787	-3.75E-06	2.07E-08	-5.39E-11	5.25E-14	
			λ_b	0.288646981	-0.026900813	0.000212298	-7.41E-07	1.58E-09	-2.06E-12	1.25E-15	
			λ_g	0.119652903	-0.031712235	0.000260052	-8.94E-07	1.57E-09	-1.39E-12	4.91E-16	
	10	Wind1	1	λ_h	-0.018057871	-0.000377557	-0.000140871	1.79E-06	-9.01E-09	2.03E-11	-1.70E-14
				λ_b	-0.190593228	-0.008930875	8.17E-06	6.41E-07	-4.49E-09	1.14E-11	-1.01E-14
				λ_g	-0.380447742	-0.015346001	0.000118835	-2.39E-07	-8.97E-10	4.20E-12	-4.47E-15
		2	λ_h	-3.620269125	0.112281354	-0.001478372	9.22E-06	-2.96E-08	4.74E-11	-2.99E-14	
			λ_b	-4.030432414	0.107086292	-0.001308216	7.39E-06	-2.07E-08	2.77E-11	-1.36E-14	
			λ_g	-4.196331979	0.09768744	-0.001127814	5.80E-06	-1.38E-08	1.33E-11	-2.25E-15	
		3	λ_h	0.870255685	-0.035282331	0.000383239	-2.32E-06	7.54E-09	-1.20E-11	7.31E-15	
			λ_b	-1.908657748	0.037327062	-0.000439988	2.22E-06	-5.37E-09	6.26E-12	-2.83E-15	
			λ_g	-2.592139763	0.048484157	-0.000573382	2.98E-06	-7.57E-09	9.32E-12	-4.48E-15	
12		Wind1	1	λ_h	0.003046098	-0.002954184	-4.77E-05	5.48E-07	-2.16E-09	3.69E-12	-2.31E-15
				λ_b	-0.179897401	-0.007866116	1.32E-05	2.14E-07	-1.20E-09	2.31E-12	-1.53E-15
				λ_g	-0.382469592	-0.01241696	6.94E-05	-1.11E-07	-2.31E-10	8.69E-13	-6.91E-16
		2	λ_h	-3527.277445	49.22217981	-0.28437734	0.000870754	-1.49E-06	1.35E-09	-5.09E-13	
			λ_b	-4066.073674	56.0114003	-0.319954463	0.000969959	-1.65E-06	1.48E-09	-5.54E-13	
			λ_g	-4223.887667	57.81457007	-0.328432188	0.000990866	-1.67E-06	1.50E-09	-5.60E-13	
		3	λ_h	-1123.405701	13.39173279	-0.065527774	0.000168289	-2.39E-07	1.79E-10	-5.48E-14	
			λ_b	-650.9073393	7.754985137	-0.037961302	9.75E-05	-1.39E-07	1.03E-10	-3.17E-14	
			λ_g	-408.154727	4.861180309	-0.02384045	6.14E-05	-8.74E-08	6.54E-11	-2.01E-14	

Table 1 — *Continued.*

Mass (M_{\odot})	Wind loss	Stage	λ	a_0	a_1	a_2	a_3	a_4	a_5	a_6	
15	Wind1	1	λ_h	-0.028115873	-0.002865229	-2.06E-05	1.88E-07	-5.34E-10	6.45E-13	-2.85E-16	
			λ_b	-0.189058198	-0.006845831	1.38E-05	6.09E-08	-2.87E-10	4.01E-13	-1.89E-16	
			λ_g	-0.384916072	-0.0111889	5.15E-05	-8.88E-08	2.15E-11	8.41E-14	-6.07E-17	
		2	λ_h	-43390.80866	415.5416274	-1.652720808	0.003494469	-4.14E-06	2.61E-09	-6.84E-13	
			λ_b	-38341.9421	366.9224492	-1.458469908	0.00308221	-3.65E-06	2.30E-09	-6.03E-13	
			λ_g	-30256.13593	289.1537559	-1.14796062	0.002423327	-2.87E-06	1.81E-09	-4.72E-13	
		3	λ_h	401.3761414	-3.338142889	0.011206254	-1.93E-05	1.77E-08	-7.96E-12	1.27E-15	
			λ_b	511.5727996	-4.483039299	0.016065894	-3.01E-05	3.11E-08	-1.67E-11	3.61E-15	
			λ_g	756.3447803	-6.901553717	0.025936812	-5.15E-05	5.69E-08	-3.32E-11	7.97E-15	
18	Wind1		λ_h	-0.011555316	-0.00112965	-3.41E-05	1.73E-07	-3.37E-10	2.89E-13	-9.07E-17	
			λ_b	-1.93E-01	-0.005828186	1.91E-06	5.64E-08	-1.57E-10	1.58E-13	-5.41E-17	
			λ_g	-4.28E-01	-0.010179044	3.42E-05	-4.69E-08	4.25E-12	3.87E-14	-2.07E-17	
		Wind2	λ_h	-0.085914616	0.000704026	-4.89E-05	2.11E-07	-3.67E-10	2.83E-13	-7.97E-17	
			λ_b	-0.218521071	-0.004292671	-1.54E-05	1.15E-07	-2.30E-10	1.90E-13	-5.53E-17	
			λ_g	-0.40399817	-0.009339995	1.81E-05	1.74E-08	-9.16E-11	9.45E-14	-3.03E-17	
	20	Wind1		λ_h	3.33E-02	-2.77E-03	-1.69E-05	9.48E-08	-1.77E-10	1.40E-13	-4.02E-17
				λ_b	-0.236292531	-4.92E-03	-6.45E-07	4.58E-08	-1.07E-10	9.55E-14	-2.93E-17
				λ_g	-0.57266423	-0.006998902	1.41E-05	1.46E-09	-4.40E-11	5.30E-14	-1.86E-17
		Wind2	λ_h	-0.084425289	-0.000248147	-3.41E-05	1.34E-07	-2.05E-10	1.36E-13	-3.30E-17	
			λ_b	-0.352025741	-0.001677298	-2.49E-05	1.09E-07	-1.72E-10	1.16E-13	-2.83E-17	
			λ_g	-0.684632138	-0.00347904	-1.36E-05	7.81E-08	-1.30E-10	9.01E-14	-2.21E-17	
25		Wind1		λ_h	-0.079805635	-0.001539374	-1.62E-05	6.42E-08	-9.17E-11	5.65E-14	-1.26E-17
				λ_b	-0.217137659	-0.005291635	4.59E-06	1.57E-08	-3.82E-11	2.89E-14	-7.22E-18
				λ_g	-0.445989682	-0.009416417	2.67E-05	-3.53E-08	1.83E-11	-7.71E-16	-1.27E-18
		Wind2	λ_h	-1.21E-01	-7.73E-04	-2.46E-05	8.75E-08	-1.17E-10	6.73E-14	-1.40E-17	
			λ_b	-2.26E-01	-4.80E-03	-2.55E-06	3.71E-08	-6.20E-11	3.94E-14	-8.66E-18	
			λ_g	-4.07E-01	-9.64E-03	2.31E-05	-2.12E-08	1.77E-12	6.23E-15	-2.05E-18	
	30	Wind1		λ_h	-0.068721052	-0.004439298	7.66E-06	-5.86E-09	-9.70E-13	3.75E-15	-1.41E-18
				λ_b	-0.168597281	-0.008185857	2.91E-05	-5.99E-08	6.65E-11	-3.71E-14	8.18E-18
				λ_g	-0.360619104	-0.013289713	5.80E-05	-1.33E-07	1.57E-10	-9.18E-14	2.10E-17
		Wind2	λ_h	-2.64E-02	-8.04E-03	3.08E-05	-6.72E-08	7.72E-11	-4.41E-14	9.86E-18	
			λ_b	-1.16E-01	-1.10E-02	4.60E-05	-1.02E-07	1.18E-10	-6.72E-14	1.50E-17	
			λ_g	-2.79E-01	-1.57E-02	7.00E-05	-1.58E-07	1.83E-10	-1.04E-13	2.30E-17	
35		Wind1		λ_h	-0.086834231	-0.005683759	1.61E-05	-2.79E-08	2.67E-11	-1.29E-14	2.48E-18
				λ_b	-0.178466739	-0.008221884	2.75E-05	-5.09E-08	4.98E-11	-2.42E-14	4.64E-18
				λ_g	-0.368625486	-0.012306112	4.58E-05	-8.80E-08	8.71E-11	-4.25E-14	8.12E-18
		Wind2	λ_h	4.10E-03	-1.07E-02	4.09E-05	-8.02E-08	8.04E-11	-3.95E-14	7.55E-18	
			λ_b	-0.082606521	-1.23E-02	4.72E-05	-9.18E-08	9.13E-11	-4.46E-14	8.48E-18	
			λ_g	-0.244193403	-0.01566844	6.06E-05	-1.17E-07	1.15E-10	-5.57E-14	1.05E-17	
	40	Wind1		λ_h	-0.113572735	-0.006236406	1.80E-05	-2.96E-08	2.58E-11	-1.13E-14	1.94E-18
				λ_b	-0.183810999	-0.008309639	2.59E-05	-4.35E-08	3.81E-11	-1.66E-14	2.83E-18
				λ_g	-0.349966999	-0.012034168	4.03E-05	-6.88E-08	6.05E-11	-2.62E-14	4.45E-18
		Wind2	λ_h	1.44E-03	-1.08E-02	3.30E-05	-5.04E-08	3.92E-11	-1.49E-14	2.21E-18	
			λ_b	-1.10E-01	-1.12E-02	3.43E-05	-5.22E-08	4.05E-11	-1.55E-14	2.30E-18	
			λ_g	-3.19E-01	-1.28E-02	3.90E-05	-5.91E-08	4.58E-11	-1.75E-14	2.62E-18	
45		Wind1		λ_h	-0.09033098	-0.0078733	2.16E-05	-3.12E-08	2.35E-11	-8.79E-15	1.29E-18
				λ_b	-0.165033235	-0.00897789	2.51E-05	-3.64E-08	2.74E-11	-1.03E-14	1.50E-18
				λ_g	-0.334563352	-0.011618318	3.36E-05	-4.94E-08	3.75E-11	-1.40E-14	2.06E-18
		Wind2	λ_h	-5.84E-02	-9.31E-03	2.27E-05	-2.86E-08	1.87E-11	-6.06E-15	7.70E-19	
			λ_b	-1.76E-01	-9.24E-03	2.22E-05	-2.76E-08	1.79E-11	-5.77E-15	7.29E-19	
			λ_g	-4.28E-01	-9.41E-03	2.14E-05	-2.57E-08	1.62E-11	-5.09E-15	6.30E-19	
	50	Wind1		λ_h	-0.077847412	-0.008264901	2.00E-05	-2.52E-08	1.65E-11	-5.39E-15	6.94E-19
				λ_b	-0.173570298	-0.008589709	2.07E-05	-2.60E-08	1.71E-11	-5.58E-15	7.20E-19
				λ_g	-0.387442471	-0.009858782	2.40E-05	-3.02E-08	1.99E-11	-6.55E-15	8.51E-19
		Wind2	λ_h	-7.61E-01	-3.18E-03	4.45E-06	-4.66E-09	3.00E-12	-9.92E-16	1.29E-19	
			λ_b	-8.68E-01	-2.98E-03	3.68E-06	-3.56E-09	2.26E-12	-7.58E-16	1.00E-19	
			λ_g	-1.18E+00	-2.19E-03	5.71E-07	8.88E-10	-7.72E-13	2.32E-16	-2.38E-20	
60		Wind1		λ_h	-0.137506172	-0.008191471	2.72E-05	-5.69E-08	6.76E-11	-4.18E-14	1.04E-17
				λ_b	-0.232113077	-0.008216679	2.75E-05	-5.78E-08	6.90E-11	-4.28E-14	1.07E-17
				λ_g	-0.475332579	-0.008678247	3.00E-05	-6.42E-08	7.76E-11	-4.86E-14	1.22E-17
		Wind2	λ_h	-0.777181069	-0.002255006	-2.51E-06	9.08E-09	-8.60E-12	3.46E-15	-5.13E-19	
			λ_b	-0.843092017	-0.002433256	-2.10E-06	8.63E-09	-8.34E-12	3.39E-15	-5.04E-19	
			λ_g	-1.055314774	-0.00279245	-2.09E-06	9.46E-09	-9.29E-12	3.80E-15	-5.66E-19	

Stage 1 begins at the exhaustion of central hydrogen and ends when the star starts to shrink (i.e., near the ignition of central He). Stage 2 is the following shrinking phase, and in Stage 3 the star expands again, until the end of the evolution.

In Table 1, we list the fitting parameters. We use the coefficient of determination \mathcal{R}^2 (i.e., the ratio of the regression sum of squares to the total sum of squares) to evaluate the goodness of fit: $\mathcal{R}^2 = 1$ corresponds to a perfect fit, while $\mathcal{R}^2 = 0$ indicates that the equation does not fit the

data at all. In our fitting results, the values of \mathcal{R}^2 in all the cases are above 0.95.

4 CONCLUSIONS

The binding energy parameter λ is a key parameter in the formation and evolution of close binary systems. This work is an updated version of Xu & Li (2010a,b), with more self-consistent treatments in stellar modeling. The main results are summarized as follows:

- (1) The λ -values vary when a star evolves and strongly depends on the star's initial mass. They generally decrease with increasing stellar radius, but rise at the very end of evolution for stars less massive than $\sim 30 M_{\odot}$.
- (2) More massive stars tend to have smaller λ . For massive stars ($\gtrsim 15 M_{\odot}$) the λ -values are substantially influenced by wind mass loss.
- (3) Generally, λ_h is several times larger than λ_b and λ_g , which can assist the ejection of the CE. For stars in the mass range of $\sim 3 - 10 M_{\odot}$, the λ_h -values can be very large (> 100) and even negative before the star reaches its maximum size.
- (4) Our fitting formulae for λ s can serve as useful input parameters in population synthesis investigations.

Acknowledgements We are grateful to an anonymous referee for helpful comments. This work was funded by the National Natural Science Foundation of China (Grant Nos. 11133001 and 11333004), and the Strategic Priority Research Program of CAS (Grant No. XDB09000000).

References

- Davis, P. J., Kolb, U., & Knigge, C. 2012, *MNRAS*, 419, 287
- de Kool, M. 1990, *ApJ*, 358, 189
- De Marco, O., Passy, J.-C., Moe, M., et al. 2011, *MNRAS*, 411, 2277
- Dewi, J. D. M., & Tauris, T. M. 2000, *A&A*, 360, 1043
- Eggleton, P. P. 1971, *MNRAS*, 151, 351
- Hamann, W.-R., & Koesterke, L. 1998, *A&A*, 335, 1003
- Hamann, W.-R., Koesterke, L., & Wessolowski, U. 1995, *A&A*, 299, 151
- Han, Z., Podsiadlowski, P., & Eggleton, P. P. 1994, *MNRAS*, 270, 121
- Hurley, J. R., Pols, O. R., & Tout, C. A. 2000, *MNRAS*, 315, 543
- Iben, Jr., I., & Livio, M. 1993, *PASP*, 105, 1373
- Ivanova, N. 2011, *ApJ*, 730, 76
- Ivanova, N., & Chaichenets, S. 2011, *ApJ*, 731, L36
- Ivanova, N., Justham, S., Chen, X., et al. 2013, *A&A Rev.*, 21, 59
- Justham, S., Rappaport, S., & Podsiadlowski, P. 2006, *MNRAS*, 366, 1415
- Kudritzki, R. P., & Reimers, D. 1978, *A&A*, 70, 227
- Nieuwenhuijzen, H., & de Jager, C. 1990, *A&A*, 231, 134
- Paxton, B., Bildsten, L., Dotter, A., et al. 2011, *ApJS*, 192, 3
- Paxton, B., Cantiello, M., Arras, P., et al. 2013, *ApJS*, 208, 4
- Paxton, B., Marchant, P., Schwab, J., et al. 2015, *ApJS*, 220, 15
- Podsiadlowski, P., Rappaport, S., & Han, Z. 2003, *MNRAS*, 341, 385
- Taam, R. E., & Sandquist, E. L. 2000, *ARA&A*, 38, 113
- Vassiliadis, E., & Wood, P. R. 1993, *ApJ*, 413, 641
- Vink, J. S., de Koter, A., & Lamers, H. J. G. L. M. 2001, *A&A*, 369, 574
- Wang, C., Jia, K., & Li, X.-D. 2016, *MNRAS*, 457, 1015
- Webbink, R. F. 1984, *ApJ*, 277, 355
- Webbink, R. F. 2008, in *Astrophysics and Space Science Library*, 352, eds. E. F. Milone, D. A. Leahy, & D. W. Hobill, 233
- Wong, T.-W., Valsecchi, F., Ansari, A., et al. 2014, *ApJ*, 790, 119
- Xu, X.-J., & Li, X.-D. 2010a, *ApJ*, 722, 1985
- Xu, X.-J., & Li, X.-D. 2010b, *ApJ*, 716, 114